JOURNAL OF GEOPHYSICAL RESEARCH, VOL. 113, A00A13, doi:10.1029/2008JA013137, 2008

Click Here for Full Article

Parameters of large-scale TEC disturbances during the strong magnetic storm on 29 October 2003

N. P. Perevalova,[1] E. L. Afraimovich,[1] S. V. Voeykov,[1] and I. V. Zhivetiev[2]

Received 29 February 2008; revised 29 July 2008; accepted 26 August 2008; published 20 November 2008.

[1] The total electron content (TEC) data obtained by the GPS network and GPS radio interferometry methods developed by the authors has made it possible to determine the spatial structure and dynamics parameters of large-scale traveling ionospheric disturbances (LS TID) generated during the strong magnetic storm on 29 October 2003. It was shown that the LS TID registered in the auroral zone after a sudden storm commencement (SSC) represented a large-scale solitary type wave with an annular front shape whose center was located near the geomagnetic pole. The wave had a period of about 40–60 min and traveled up to 4500 km equatorward. The relative amplitude of the LS TID was 5–10%. Comparison with ionosonde data has shown that this value corresponds to the relative amplitude of electron density disturbance in the *F* layer maximum of about 45–50%. The velocity and travel direction of the LS TID had a strongly pronounced longitudinal dependence. A ''swirling'' effect was detected in the LS TID movement, the direction of which was opposite to the Earth's rotation. The westward directed zonal projection of LS TID velocity caused this ''swirling'' effect. In the morning and evening sectors the zonal projection exceeded the meridional one. The diurnal movement of the ionization maximum may influence the zonal transfer of LS TID.

Citation: Perevalova, N. P., E. L. Afraimovich, S. V. Voeykov, and I. V. Zhivetiev (2008), Parameters of large-scale TEC disturbances during the strong magnetic storm on 29 October 2003, *J. Geophys. Res.*, *113*, A00A13, doi:10.1029/2008JA013137.

1. Introduction

[2] The geophysical effects of magnetic storms have attracted persistent interest for a long time. Most major features of the magnetosphere and ionosphere change during strong geomagnetic disturbances. The ionospheric response to a magnetic storm depends on a great number of parameters: location of the observation station, season, solar activity phase, time of storm onset, etc. Many publications have been devoted to the study of large-scale traveling ionospheric disturbances (LS TIDs) generated during a magnetic storm in the auroral zone (see reviews by *Hocke and Schlegel* [1996] and *Oliver et al.* [1997]). Research on LS TIDs can provide important information about processes in this zone under quiet and disturbed conditions. However, the basic properties and parameters of LS TIDs are still imperfectly understood. Are they a periodic process or a solitary wave propagating large distances from the source of its generation? What is the shape and width of the wavefront of LS TIDs? What is these LS TIDs' propagation direction? Why did investigators report markedly differing propagation velocities for LS TIDs generated in the auroral zone? Solving these questions requires an appropriate spatial-temporal resolution which cannot be provided by existing highly sparse networks of ionosonde, incoherent scatter radars and MST-radars.

[3] The highly dense GPS network represents a unique instrument for sounding the upper atmosphere. Investigations of the upper atmosphere using the international GPS network have lately been widespread. These investigations rely on determining the total electron content (TEC), which is calculated from measurements of phase path increments of the GPS transionospheric radio signals. Many publications have been devoted to the study of the effects of powerful geomagnetic storms on 29–30 October 2003 [*Afraimovich et al.*, 2004, 2006; *Mannucci et al.*, 2005; *Foster and Rideout*, 2005; *Zhao et al.*, 2005; *Ding et al.*, 2007; *Afraimovich et al.*, 2008]. A large increase in the dayside TEC at low and middle latitudes was a main ionospheric manifestation of these events [*Mannucci et al.*, 2005; *Foster and Rideout*, 2005; *Zhao et al.*, 2005]. LS TIDs propagating equatorward in the range 60–30°N were observed on 29–30 October 2003 in different longitudinal sectors [*Afraimovich et al.*, 2004, 2006; *Ding et al.*, 2007; *Afraimovich et al.*, 2008]. A detailed study of storm-time LS TID parameters (including the mapping of TEC perturbations [*Ding et al.*, 2007]) was performed relying on the dense GPS network over North America. In this paper we present the results of a comprehensive investigation of LS TIDs generated in auroral zone after the sudden storm commencement (SSC) of a magnetic storm on 29 October 2003. We used available data from all GPS receivers in the

[1]Institute of Solar-Terrestrial Physics, Russian Academy of Sciences, SB RAS, Irkutsk, Russia.
[2]Institute of Cosmophysical Research and Radiowave Propagation, Russian Academy of Sciences, FEB RAS, Paratunka, Russia.

Copyright 2008 by the American Geophysical Union.
0148-0227/08/2008JA013137$09.00

northern hemisphere encircling the globe as well as the original methods, we developed, for determining of LS TID parameters. All data were processed by the same methods. Such an approach provides new information about the spatial structure and dynamics parameters of storm-time LS TIDs.

2. Data and Measurement Methods

[4] The investigation of large-scale traveling ionospheric disturbances (LS TID) during the magnetic storm on 29 October 2003 was based on phase measurements of the total electron content (TEC) by the international GPS network. We used data from GPS receivers in five sectors of the northern hemisphere: West American (sector A), East American (sector B), European (sector C), Asian (sector D) and Far Eastern (sector E). The sequence of data processing procedures was as follows. Series of "oblique" TEC I_0 (t) along the receiver-satellite lines of sight (LOSs) were calculated from the data of dual-frequency phase measurements by GPS receivers [*Hofmann-Wellenhof et al.*, 1992]. The generally accepted TEC unit is TECU (Total Electron Content Unit), which is equal to 10^{16} m^{-2}. We chose continuous series I_0 (t) with a time duration of no less than 3 h. These series as well as the corresponding series of LOS elevation θ_S (t) and LOS azimuth α_S (t) constituted the input data. The initial TEC series were converted to an equivalent "vertical" I(t) value [*Klobuchar*, 1987], to normalize of the amplitude of TEC disturbances (data for satellite elevation larger than 30° were used). Next the TEC variations dI(t) were calculated by smoothing the I(t)-series with a selected time window of 30 min and removing the linear trend with a window of about 60 min. Thus, we filtered the TEC variations in the period range 30–60 min corresponding to the LS TID periods. The LS TID horizontal phase velocity V_h and azimuth α were calculated using the algorithm SADM-GPS of the GPS interferometry developed at the Institute of Solar-Terrestrial Physics SB RAS [*Afraimovich et al.*, 2000]. The algorithm is based on calculating V_h and α using TEC spatial (I'_x, I'_y) and temporal (I'_t) derivatives from TEC measurements at three spaced GPS stations (GPS-array). In the first approximation LS TID may be represented as a traveling plane wave $I(t, x, y) = I_0 \sin(\Omega t - K_x x - K_y y + \varphi_0)$, where I_0, φ_0 are the amplitude and initial phase, K_x, K_y, Ω are the x and y projections of the wave vector **K**, and the angular frequency, respectively. For this LS TID model it is possible to determine the azimuth and horizontal phase velocity by formulas [*Afraimovich et al.*, 2000]:

$$\alpha(t) = \mathrm{arctg}\left(K_x/K_y\right) = \mathrm{arctg}\left(I'_x/I'_y\right)$$
$$V_h = \frac{I'_t}{\sqrt{I'^2_x + I'^2_y}} + W_x \sin\alpha + W_y \cos\alpha, \quad (1)$$

where W_x and W_y are the projections of the velocity of an ionospheric point (to account for the satellite motion). The ionospheric point is where the LOS crosses the horizontal plane at the height h_{max} of the maximum of the ionospheric F_2 region. h_{max} varies 250–400 km depending on time, season, latitudes etc. To simplify calculation we used h_{max} = 300 km for all conditions.

[5] The intensity of LS TID registered by GPS receivers during the magnetic storms on 29 October 2003 was compared with that of local electron density (Ne) disturbances. For this purpose we used measurements of the critical frequency of the ionospheric F_2 region f_0F_2 at the Irkutsk Digisonde DPS-4 (52.2°N; 104.3°E). As is well known, f_0F_2 is related to electron density in the maximum of the ionospheric F_2 region Ne_{max} [*Ratcliffe*, 1959]: $f_0F_2 = \sqrt{e^2 Ne_{max}/\pi m_e}$ (where e is the electron charge, m_e is the electron mass). Thus f_0F_2 variations are effects of Ne disturbances.

[6] To define the general ionospheric response to the magnetic storm on 29 October 2003 we used data of Global Ionospheric Maps (GIM). GIM are global maps of absolute "vertical" TEC value I_A created by interpolation of international GPS network data [*Mannucci et al.*, 1998]. GIM are generated in a special IONEX format and contain the TEC value at longitudinal-latitudinal grid nodes. The spatial range of standard GIM is 180°W–180°E longitude and 87.5°S–87.5°N latitude. The spatial resolution is 5° longitude and 2.5° latitude; the time resolution is 2 h. GIM are produced daily by several scientific centers (for example, the Center for Orbit Determination in Europe, University of Berne, Switzerland (CODG, http://www.cx.unibe.ch), Jet Propulsion Laboratory of California Institute of Technology (JPLG, http://www.jpl.nasa.gov) and are available at ftp://cddisa.gsfc.nasa.gov/pub/gps/products/ionex.

[7] We employed data of the magnetic stations Victoria (48.5°N; 236.6°E), Ottawa (45.4°N; 284.5°E), Hel (54.6°N; 18.8°E), Irkutsk (52.2°N; 104.5°E) and Paratunka (53.0°N; 158.3°E) for geomagnetic situation control and time calibration. The data of the Space Environmental Monitor (SEM, http://www.sec.noaa.gov/pmap) were used to mark the displacement and dynamics of the auroral oval.

3. Ionospheric Response to the Magnetic Storm on 29 October 2003 as Deduced From GIM

[8] The left side of Figure 1 presents vertical TEC maps at 0800 UT and 1000 UT on 29 October 2003 in the northern hemisphere at polar coordinates, based on GIM data. GIM for the same times on a magnetically quiet day 23 October 2003 are on the right. The TEC maps show global-scale features and dynamics of TEC variations in the ionosphere. Both in quiet and disturbed conditions the daily motion of ionization are well traceable on the maps. The ionization maximum is observed near 1400 LT and the minimum near 0400 LT. The equatorial anomaly is very manifest. In quiet conditions the northern crest of the anomaly is observed at latitudes 10–17° in the morning, day time and evening sectors. The TEC value in the crest does not exceed 80 TECU. During the magnetic storm the northern crest of the equatorial anomaly was displaced northward up to latitudes 20–22°. This effect is in good agreement with results obtained by *Astafyeva et al.* [2007]. The TEC value in the crest increases up to 130 TECU. At the same time, the main ionospheric trough (one of the most important large-scale formations in the ionosphere) is not visible in GIM. It is not possible to detect LS TIDs in GIM

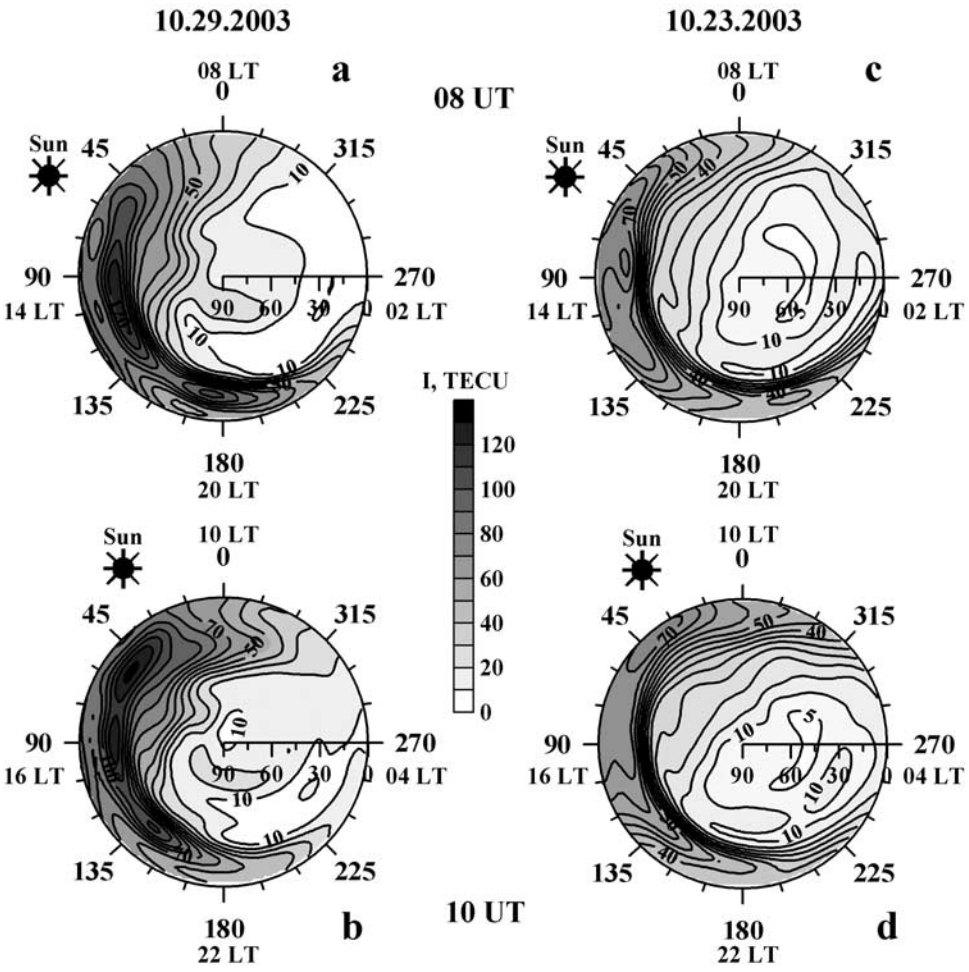

Figure 1. Global Ionospheric Maps of vertical TEC I in the northern hemisphere (a and b) for the magnetically quiet day of 23 October 2003 and (c and d) during the geomagnetic storm on 29 October 2003. "Sun" marks the local noon.

data, although such disturbances were registered by GPS receivers (see below).

[9] For details we have constructed Global Maps of TEC Relative Deviation ΔI (Figure 2):

$$\Delta I = 100\% \cdot (I_{29} - I_{23})/I_{23}, \quad (2)$$

where I_{29}, I_{23} are GIM TEC values for 29 October 2003 and 23 October 2003, respectively.

[10] Until the SSC, TEC values on 29 October 2003 exceeded, as a whole, those on the quiet day (Figure 2a), although a few small regions with decreased TEC existed. This pattern most probably arises from higher magnetic activity. After the storm onset, the spatial distribution of TEC deviations has a characteristic form. It is possible to select two large areas with increased TEC values (Figure 2b). Along the crest of the equatorial anomaly, the TEC increase is 150–200% in comparison with the quiet level. At high latitudes in the night hemisphere, the TEC increases up to 400%. The area of the high-latitude TEC increase mimics the shape of the southern boundary of the auroral oval (Figure 2b). An essential (up to 50–100%) decrease in TEC values is observed in the night ionosphere at mid and low latitudes. The above described distribution of TEC deviation is stationary enough and does not vary for several hours. It is not possible to select LS TID on maps of TEC deviation.

[11] Unfortunately, the spatial-time resolution of standard GIM appears to be insufficient for detection of medium- to small-scale ionospheric disturbances. It should be remembered that the precision of TEC interpolation depends on the number of GPS sites in different regions. In the Asian, Pacific and Atlantic regions, the distances between GPS receivers are hundreds to thousands of kilometers. GPS sites are absent at latitudes of more than 80°. In these regions, TEC interpolation can smooth out small-scale features. *Ho et al.* [1996] reported TID observed using TEC deviation maps during the geomagnetic storm on 26 November 1994. However, they used maps with a time interval of 15 min. The time resolution of standard GIM is 2 h. *Ho et al.* [1996] identified TID as a large region (extending from 70°N to 40°N and more than 70° in longitude) with increased TEC compared to those under quiet conditions. This region existed and expanded for more than 4 h. We regarded TIDs as wave structures with periods of 30–120 min and wave-

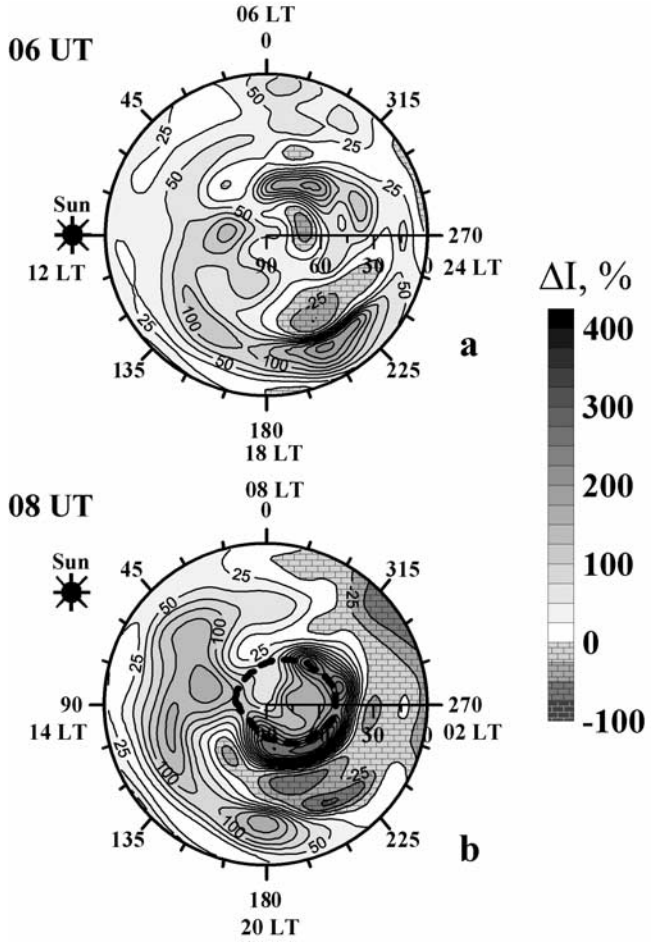

Figure 2. Global Maps of TEC Relative Deviation ΔI at 0600 and 0800 UT. The dashed line marks the position of the southern boundary of the auroral oval for 0642 UT on 29 October 2003 (Figure 2b).

lengths of 500–1000 km. Thus we term different objects as TIDs from those studied by *Ho et al.* [1996].

4. LS TID Features as Deduced From GPS Data for 29 October 2003

[12] Dots on Figure 3 show the positions of the GPS receivers whose data were used to investigate ionospheric disturbances generated by the magnetic storm on 29 October 2003. The longitudinal sectors are designated as regions A, B, C, D, and E. Squares mark the location of the magnetic stations. The thick dashed line marks the position of the southern boundary of the auroral oval for 0526 UT on 29 October 2003 (http://www.sec.noaa.gov/pmap). The position of the North Magnetic Pole (NMP) is shown by a cross.

[13] TEC wave disturbances with a time period of about 40–60 min were detected in all the sectors after the SSC (0611 UT) on 29 October 2003. The mean values of LS TID parameters for each sector are given in Table 1, where A_I and T_I are the LS TID amplitude and period, V_h and α are the horizontal velocity and azimuth of the LS TID propagation calculated by the SADM-GPS algorithm, σV_h and $\sigma\alpha$ are the r.m.s. of the horizontal velocity and of the azimuth, respectively, τ is the delay between the start time of sharp TEC changes and the SSC, N is the number of TEC series.

[14] Comparison with magnetic station data has shown that the LS TID occurs during a sharp change of the horizontal component of the Earth's magnetic field. The dashed vertical line in Figure 4 marks the SSC moment and the solid vertical line shows the start time of sharp TEC changes in the dI(t) series. Intense fluctuations of the geomagnetic field H component are detected by magnetic stations in different parts of the world over 0610–1100 UT. This period coincides with the time when the maximum values of the derivative *dDst*/*dt* are present. LS TID in TEC variations are registered by the GPS receivers at the same time (hatched area in Figures 4a–4f). The delay τ between the beginning of sharp TEC changes and the SSC varied from 2 to 10 min.

[15] In the Asian sector we detected the LS TID using TEC data from GPS station IRKT and f_0F_2 measurements by the Irkutsk ionosonde. It allowed us to compare the relative amplitudes of TEC and Ne disturbances. For comparison we chose TEC series from LOSs IRKT–PRN03 and IRKT–PRN02, where PRNXX denotes the number of GPS satellite. Throughout the observation time 0600–1000 UT, PRN03 and PRN02 had the highest elevations of all the visible GPS satellites. The ionospheric

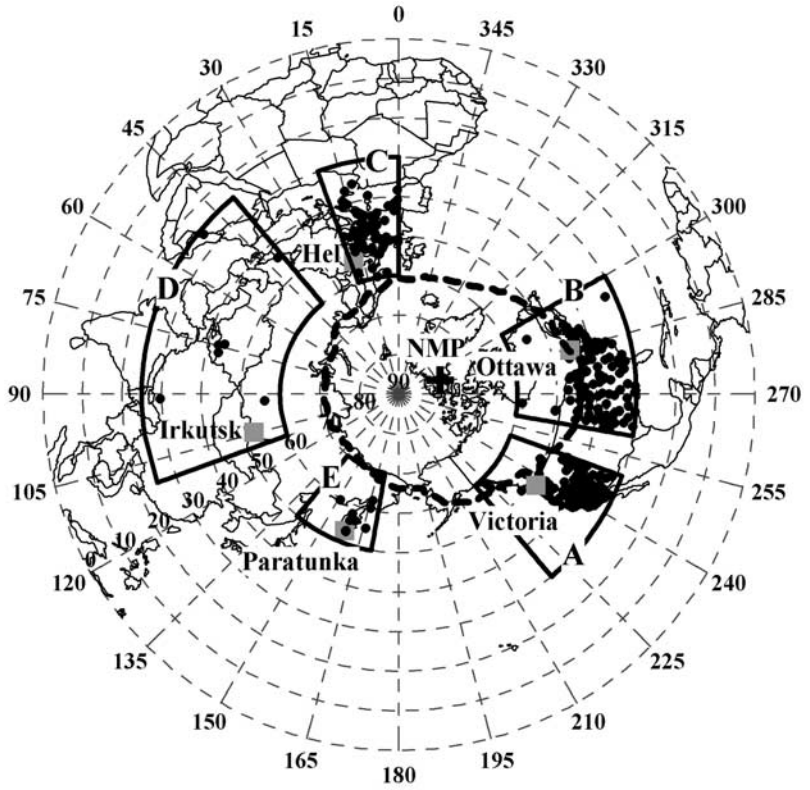

Figure 3. The geometry of measurements on 29 October 2003. Dots stand for the GPS receivers; squares stand for the magnetic stations. The dashed line marks the position of the southern boundary of the auroral oval for 0642 UT on 29 October 2003.

points of two selected LOSs were nearest to the reflection point of the ionosonde signal (i.e., to the vertical). The initial TEC series were converted to the "vertical" value and filtered in the range of periods 30–120 min by procedures described in section 2. The gray lines in Figure 5 show the filtered "vertical" TEC variations dI(t) at LOSs IRKT–PRN03 (solid line) and IRKT–PRN02 (dashed line). The black thick line shows the variations in the critical frequency f_0F_2. The scale of the corresponding approximate values of the electron density Ne at the F region maximum is shown on the right in Figure 5. It is obvious that the f_0F_2 variations are similar to the TEC variations in the time interval 0700 to 0800 UT. The minima of TEC and f_0F_2 variations are observed at approximately 0730 UT. By our estimations the LS TID wavelength was about 1000 km. The distances between the ionospheric points and the reflection point of the ionosonde signal were significantly less than LS TID wavelength during the entire observation time. This means that the GPS receivers and the ionosonde detected the same LS TID.

[16] The relative amplitude R_I of the TEC disturbance was calculated as $R_I = 100\% \cdot (dI_{max} - dI_{min})/I_{GIM}$, where dI_{max} and dI_{min} were the maximum and minimum values of TEC in the series dI(t) at LOSs IRKT–PRN03 and IRKT–PRN02; I_{GIM} was the value of the absolute "vertical" TEC deduced from GIM. We used I_{GIM} value in the GIM-node located near the GPS station IRKT at 0600 UT (time closed to the LS TID onset). R_I was about 5% at LOS ITKT-PRN03 (Table 2). The relative amplitude R_{Ne} of the electron density disturbance was determined as $R_{Ne} = 100\% \cdot (Ne_{max} - Ne_{min})/Ne_{max}$, where Ne_{max} and Ne_{min} were the maximum and minimum values of the electron density Ne disturbance. The observed change in the critical frequency f_0F_2 corresponds to the relative amplitude of the electron density disturbance at the F region maximum $R_{Ne} \approx 50\%$ (Table 2). Similar results were obtained during magnetic storms on 17 April 2002 [*Afraimovich et al.*, 2004], on 30 October 2003 and 10 November 2004 [*Afraimovich et al.*, 2008] (Table 2).

[17] To trace the dynamics of LS TID along its traveling directions we have introduced a special reference frame in

Table 1. LS TID Parameters in Different Longitudinal Sectors

Sector	A_I, TECU	T_I, min	V_h, m/s	σV_h, m/s	α, deg	$\sigma\alpha$, deg	τ, min	N
A West American	0.4	48	1090	364	208	7	3.4	120
B East American	1.3	48	684	310	194	30	2.2	80
C European	1.2	60	1508	540	259	46	2.8	86
D Asian	2.2	54	1640	397	194	93	3.4	7
E Far Eastern	2.5	60	1013	350	235	32	3.4	11

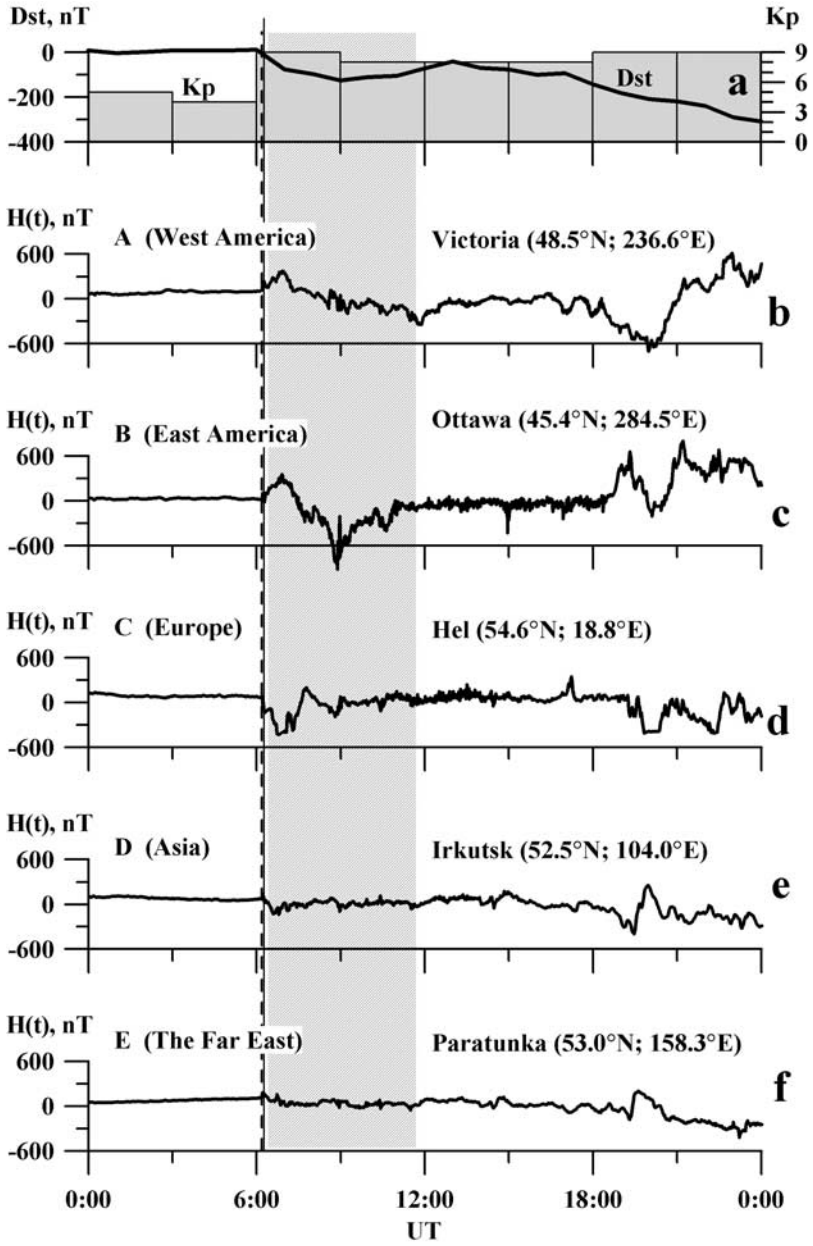

Figure 4. Variations of geomagnetic parameters during the magnetic storm on 29 October 2003: (a) the indices *Dst* and *Kp* and (b–f) the geomagnetic field H component detected by five magnetic stations.

each sector (Figure 6f). The axis of this frame runs along, but is counter directed to, the LS TID wave vector **K**. We mapped filtered TEC variations in each sector in the same graph (Figures 6a–6e) with a vertical shift proportional to distance D between the start point O and GPS receiver location (Figure 6f). The filtering method is described in section 2. In the Figures 6a–6e the first (leftmost) dot of each series corresponds to distance D of GPS receiver in which this series was detected. The scale of TEC variations is marked by a black arrow. The GPS satellite number is marked in each panel. We used TEC series from these satellites because they had the highest elevations throughout the observation time. One can see that the detected disturbance was a large-scale solitary type wave lasting about

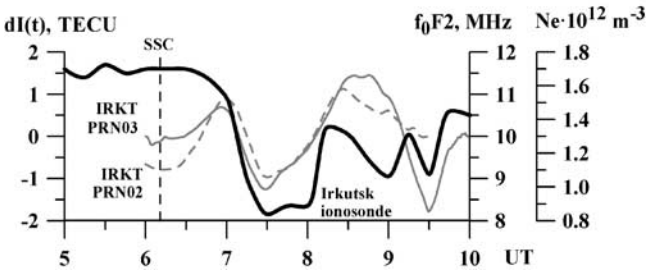

Figure 5. Comparison of TEC (gray lines) and f_0F_2 (black line) variations in the Asian sector during the magnetic storm on 29 October 2003. The scale of the values of the electron density Ne at the *F* region maximum is shown on the right.

Table 2. Relative Amplitudes R_I and R_{Ne} During Different Magnetic Storms

Magnetic Storm	*Dst*, nT	*Kp*	$dI_{max} - dI_{min}$, TECU	I_0, TECU	R_I, %	R_{Ne}, %
29 Oct 2003	−308	9	2.0–4.5	≈40	5–11	45–50
17 Apr 2002	−127	7	∼1.2	≈20	6	10–14
30 Oct 2003	−347	9	∼14	≈100	14	40
10 Nov 2004	−383	9	∼15	≈30	50	85

40 min which traveled up to 800–4500 km without changing its shape.

5. LS TID Wavefront Shape

[18] As follows from the above, LS TID with similar parameters (wave type, period, amplitude, velocity and direction of propagation) are registered in TEC variations by the GPS receivers in different longitudinal sectors within the same universal time period. It is interesting to observe the spatial distribution of TEC perturbations as well as their travel. We developed two special methods for visualization of TEC disturbances and for determination of the LS TID wavefront shape: a method for constructing of spatial TEC images and a method for TEC variation mapping.

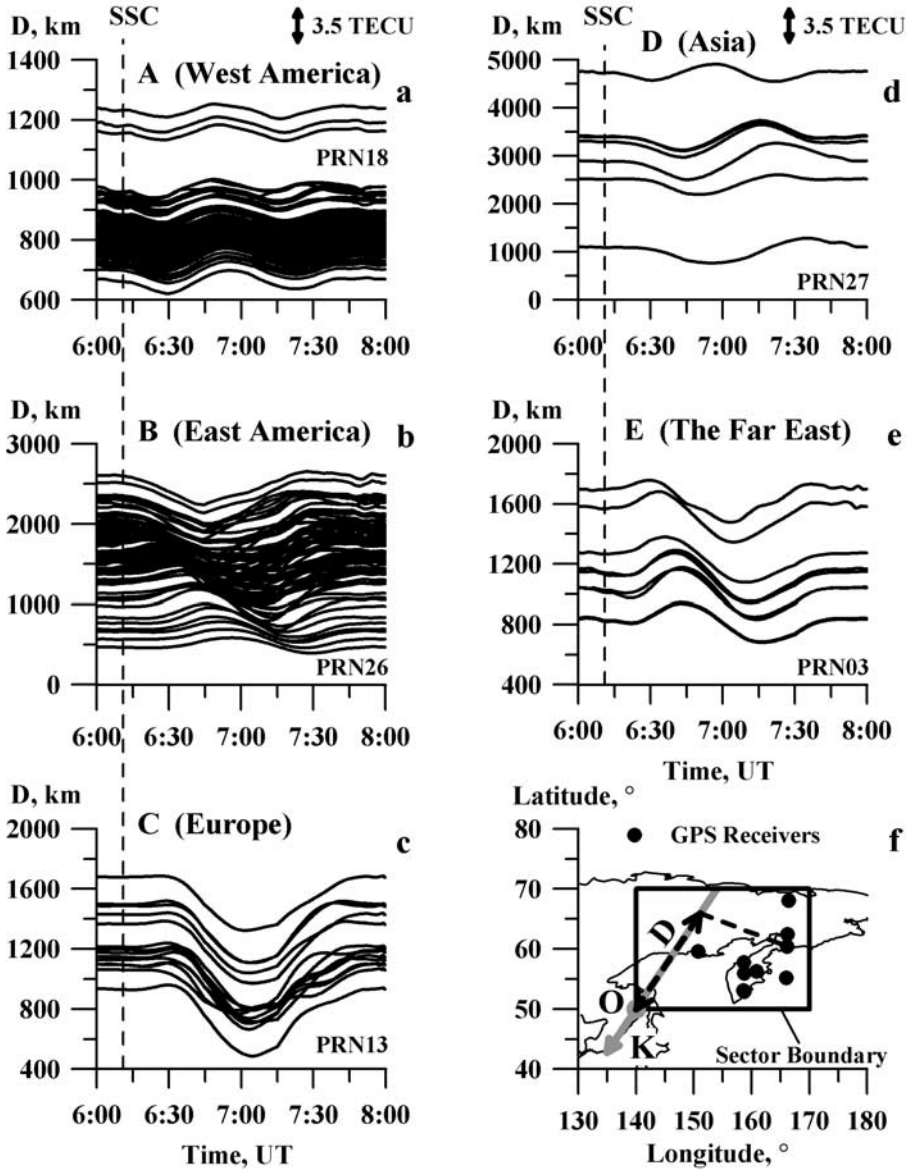

Figure 6. Temporal variations of filtered TEC in longitudinal sectors at different distances D from the start point O (Figures 6a–6e). The distance D is shown on the vertical axis. The black arrow sets the scale of TEC variations. The GPS satellite numbers are indicated. Figure 6f illustrates the determination of distance D.

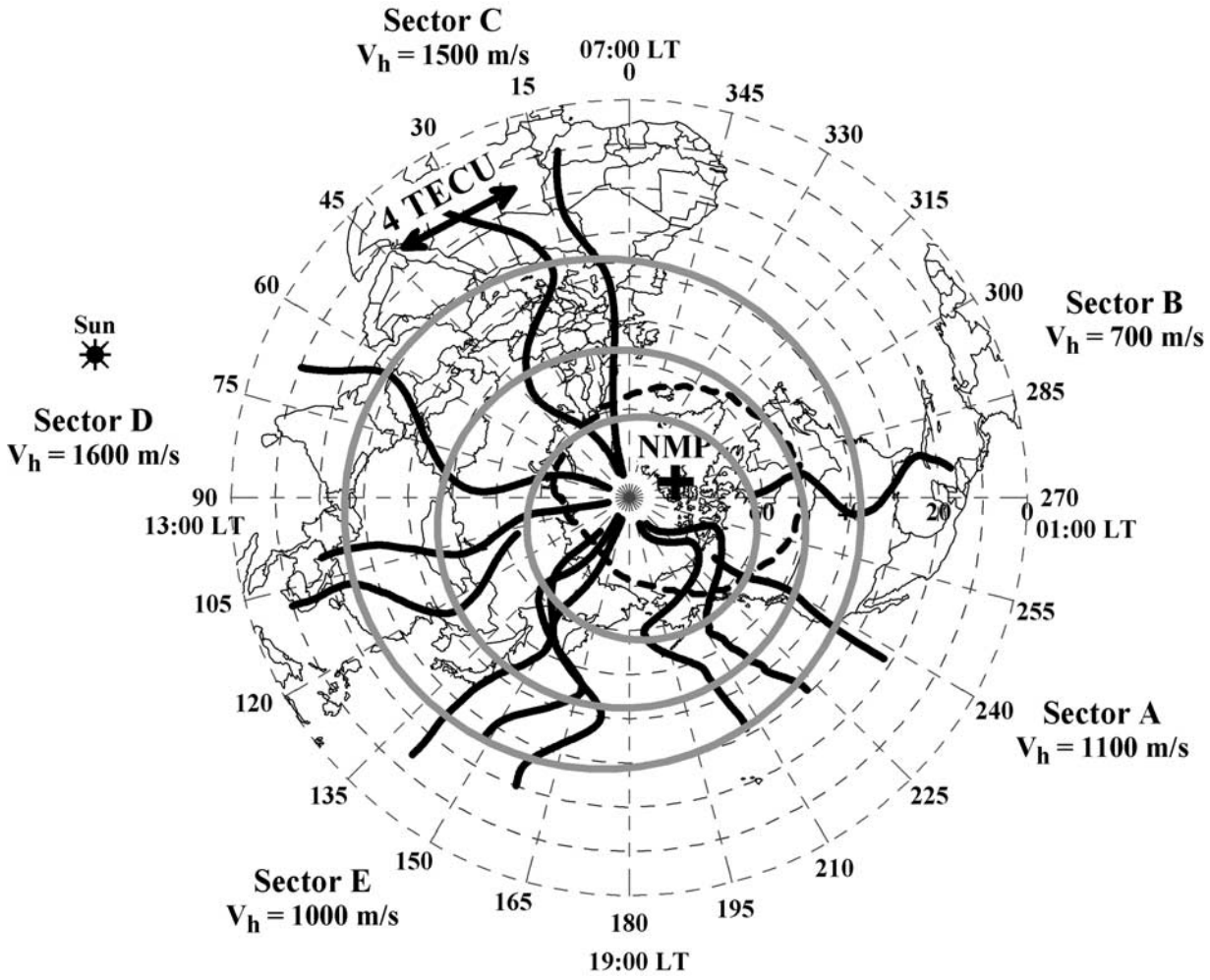

Figure 7. The LS TID wavefront shape (thick gray lines) on 29 October 2003 reconstructed using spatial TEC images (solid black curves). The thick dashed black line marks the position of the southern boundary of the auroral oval for 0642 UT on 29 October 2003.

5.1. Spatial TEC Images

[19] To reconstruct the spatial picture of TEC variations, the TEC series were represented as curves of longitude deviation from the receiver longitude (spatial TEC images). Spatial TEC images for 0700 UT are shown in Figure 7 (black curves). A black arrow marks the scale of TEC variation. For constructing spatial TEC images we used several filtered TEC series for the time interval 0600–0800 UT pictured in Figures 6a–6e. The time moment 0700 UT corresponded to the middle of the series. In each sector we randomly chose a few filtered TEC series (from 1 to 3, depending on the longitudinal size of the sector). The latitudinal extension of the spatial TEC image was calculated as the product of the average LS TID meridional velocity in the sector and the series duration. The central latitude of the image was selected as the latitude of a corresponding GPS receiver.

[20] Thick gray lines in Figure 7 mark approach positions of the maxima and minima in spatial TEC variations calculated by ellipse approximation. It turned out that the ellipse eccentricities were small (0.1–0.2), i.e., the ellipses were close to circles. One can see that the TEC disturbance generated during the magnetic storm had an annular front shape. The ring center was situated inside of the auroral oval near the geomagnetic pole. The LS TID traveled toward lower latitudes. The smallest velocity values were observed on the night side. The LS TID traveled almost without changing its annular front shape. Different velocities between the night and day sectors manifest themselves in shifting the ring center from the geomagnetic pole to the day side.

5.2. TEC Variation Mapping

[21] To map the TEC variation we calculated the amplitude of oscillations for each TEC series dI(t) filtered over a range of periods 20–60 min. The TEC variations with an amplitude exceeding 1 TECU and the specified threshold $\varepsilon = A_{max}/2$ (where A_{max} is the maximum amplitude in each TEC series) were selected. We interpreted such variations as TEC minima and TEC maxima. The time of minima and maxima were detected. Then we mapped the location of ionospheric points for receiver-satellite LOSs, where extremes in TEC variations were found. The coordinates of ionospheric points were calculated for the height h_{max} = 300 km of the F_2 layer maximum.

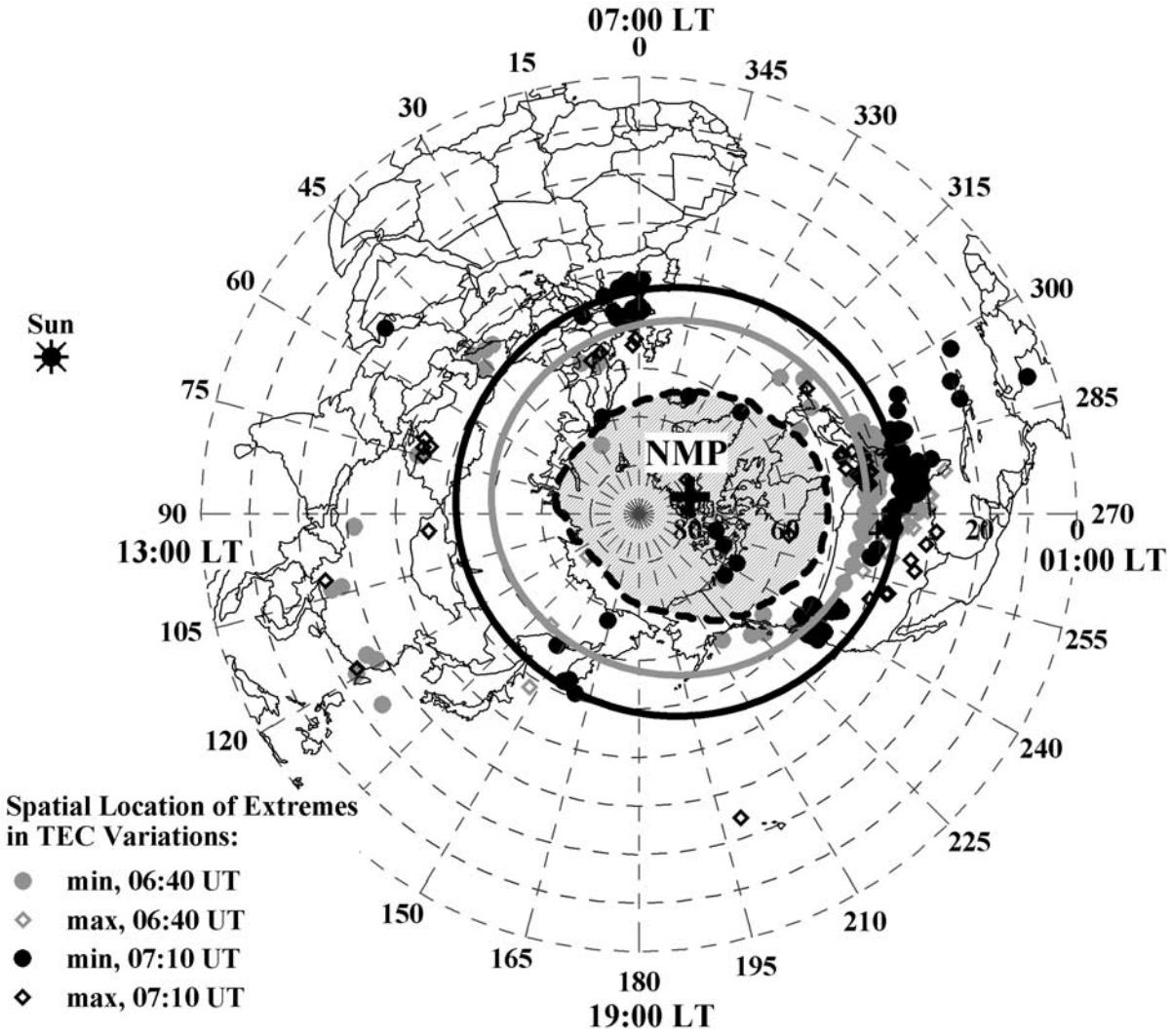

Figure 8. The LS TID wavefront shape on 29 October 2003 reconstructed using TEC variation mapping. The thick dashed black line marks the position of the southern boundary of the auroral oval for 0642 UT on 29 October 2003.

[22] Dots and diamonds in Figure 8 mark the location of ionospheric points where TEC variation minima and maxima (respectively) were detected at 0640 UT and 0710 UT. Analysis of spatial distributions of extremes in TEC variation for different times allows us both to estimate the LS TID wavefront shape and to study the dynamics of TEC variations. It is possible to distinguish two kinds of TEC disturbances in the auroral zone after the SSC. The first kind is quasi-chaotic TEC fluctuations inside of the auroral oval (hatched area in Figure 8). It is a result of local electron density disturbances in the ionosphere within this area. The second kind is a LS TID characterized as a large-scale solitary type wave with a period of about 40–60 min. This wave is continuously generated at the southern boundary of the auroral oval and travels equatorward to 20–25°N latitudes (up to 4500 km). The LS TID has an annular front shape (thick solid lines in Figure 8) whose center is located near the geomagnetic pole. The thick gray line represents the location of the LS TID at 0640 UT, the thick black line does the same for 0710 UT. Position of the front shape was calculated by ellipse approximation of minimum locations at these times. The ellipse eccentricities varied from 0.1 to 0.4 (the front shape was close to a circle). For approximation we chose minima located between 55°N and 30°N to ensure the LS TID causes them. TEC variation extremes at latitudes near and lower 20°N are not as a rule a result of auroral disturbances. It is more probable that points registered near longitudes 90–120°E and latitudes 20–25°N are generated at the northern crest of the equatorial anomaly. It should be noted that one or two LS TID crests may be observed at each time moment. In our opinion, the minima located near 45°E and 40–43°N at 0640 UT belong to a second crest of LS TID wave.

[23] It is possible to estimate the mean meridional velocity V_r of LS TID propagation from the distance the wavefront travels within 30 min (from 0640 to 0710 UT). Given that ionospheric points are located at a height of 300 km (section 2), the mean $V_r \approx 580$ m/s. Using Table 1 we can estimate the meridional projections of LS TID horizontal velocity calculated by the SADM-GPS algorithm: $V_y = V_h$

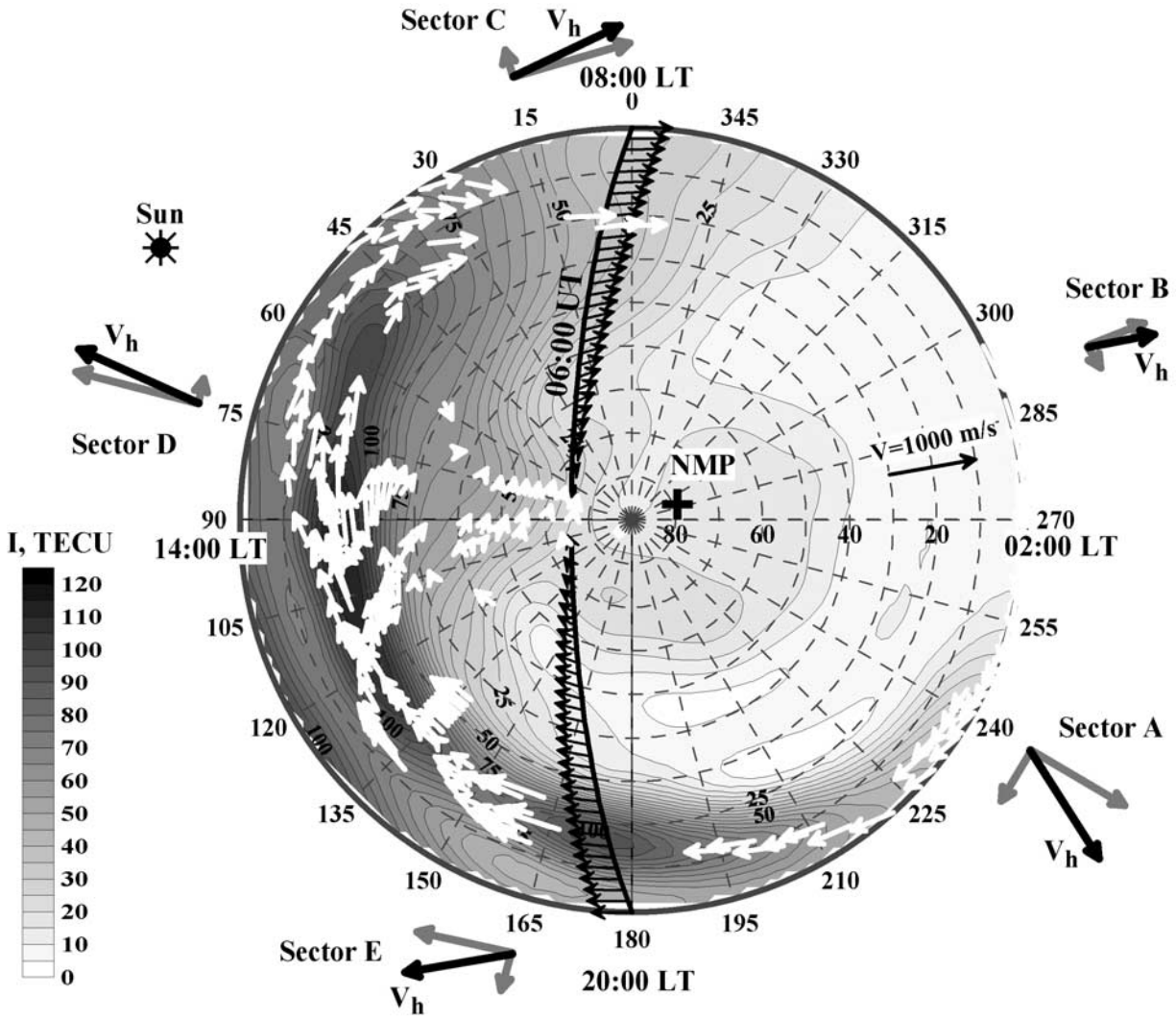

Figure 9. Comparison of the LS TID propagation (black and gray arrows on the perimeter) with the motion of TEC isolines (white arrows) on 29 October 2003. The black line with arrows shows the position and motion of the terminator for 0600 UT.

cos (α). The mean V_y value for five longitudinal sectors is 812 ± 263 m/s. V_r and V_y are quite close. The difference in the velocities as obtained by the two methods is caused both by the method accuracy and the longitudinal dependence of the V_y value (see section 6).

[24] Thus using two different methods to visualize TEC disturbances we found that the large-scale wave of the solitary type generated in the auroral zone after the SSC on 29 October 2003 had an annular front shape centered near the geomagnetic pole. The method of TEC variation mapping produced a more realistic representation of the LS TID shape and allowed us to trace the dynamics of TEC disturbances in the auroral zone.

6. LS TID Propagation

[25] Thick black arrows in Figure 9 show the directions of the horizontal LS TID velocity V_h calculated by the SADM-GPS algorithm in each sector (Table 1). They correspond to approximate trajectories of the LS TID propagation in different regions. It is obvious that the velocity and direction of the LS TID propagation depend on the longitude. Comparison with the GIM data has shown that the smallest LS TID velocity (700 m/s) is detected in the night region, where TEC values are minimum (Figure 9). The highest LS TID velocity (1600 m/s) is detected in the day side, where the value of TEC is larger (Figure 9).

[26] Gray arrows in Figure 9 show the zonal and meridional projections of the LS TID horizontal velocity. The LS TID propagates equatorward. But the wavefront behaves as if it ''swirls'' in the direction opposite to the Earth's rotation. The ''swirling'' effect is caused by the westward directed zonal projection of the LS TID horizontal velocity. In the morning and evening sectors the zonal projection exceeds the meridional one. In the night and day sectors the propagation direction becomes close to meridional.

[27] One can assume that displacement of background ionization influences the characteristics of the LS TID propagation. To check up this hypothesis we calculated the velocity and travel direction of the TEC isolines using GIM. For this purpose five special points were selected on each isoline (Figure 10e): easternmost E (with the maximum

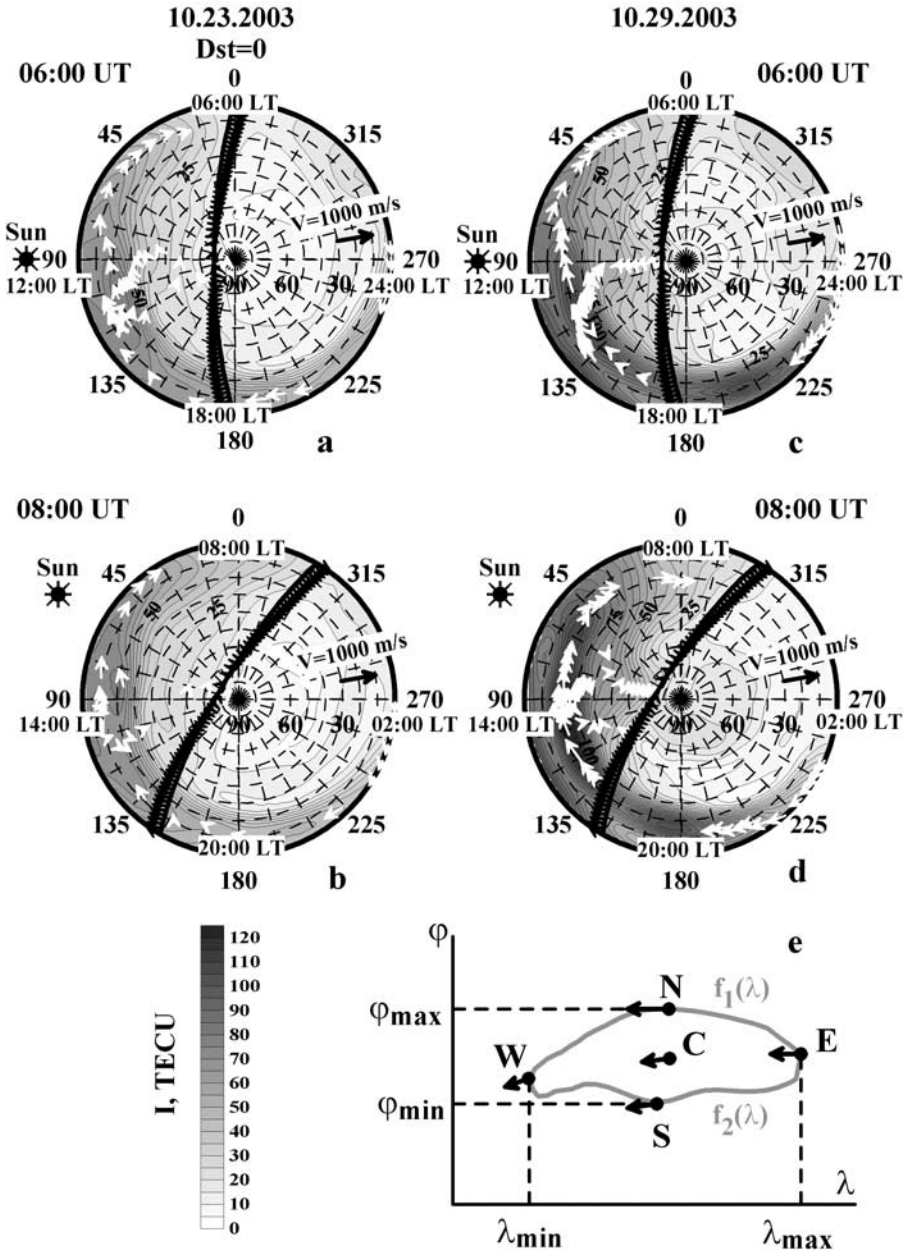

Figure 10. The motion of TEC isolines (white arrows) in (a and b) quiet and (c and d) disturbed conditions at 0600 and 0800 UT. "Sun" marks the local noon. (e) Calculation of the velocity and travel direction of TEC isolines.

longitude λ_{max}), westernmost W (with the minimum longitude λ_{min}), northernmost N (with the maximum latitude φ_{max}), southernmost S (with the minimum latitude φ_{min}) points, and the contour centroid C (with coordinates λ_C and φ_C). The centroid coordinates were calculated using the formulae for a plane figure bounded by a selected isoline:

$$\lambda_C = \frac{1}{S}\int_{\lambda_{min}}^{\lambda_{max}} \lambda \cdot [f_1(\lambda) - f_2(\lambda)]d\lambda$$
$$\varphi_C = \frac{1}{2S}\int_{\lambda_{min}}^{\lambda_{max}} [f_1^2(\lambda) - f_2^2(\lambda)]d\lambda, \quad (3)$$

where $f_1(\lambda)$ and $f_2(\lambda)$ are the "top" and "bottom" parts of the isoline, delimited by the easternmost (λ_{max}) and westernmost (λ_{min}) points (Figure 10e); S is the area of the figure enclosed by the isoline. For calculations we selected isolines which crossed any meridian at no more than two points (i.e., had no "tongue"-like curves etc.).

[28] The motion trajectory of the special points was traced and their velocity was taken as the TEC isoline velocity. On the magnetically quiet day 23 October 2003 the velocity was calculated for the 5, 10, ... 70 TECU isolines. On the magnetically disturbed day 29 October 2003 the velocity was calculated for the 25, 30, ... 105 TECU isolines at 0600 UT and the 20, 25, ... 125 TECU isolines at 0800 UT. The maps of velocities of TEC isolines

(white arrows) in quiet (Figures 10a and 10b) and disturbed (Figures 10c and 10d) conditions are presented. The black line with arrows shows the position and velocity of the terminator on the Earth's surface. The black arrow labeled V = 1000 m/s marks the velocity scale. TEC isolines travel along the parallels: in all cases the azimuth is close to 270° (the r.m.s. of the azimuth is 40°). The isoline motion velocity depends on latitude. At low (10–30°) latitudes the velocities vary from 350 m/s to 700 m/s, and at high latitudes (60–75°) they decrease down to 30–100 m/s. The terminator has a similar character of velocity variations: the terminator velocity is 463 m/s on the equator and 100 m/s at 77.5° latitude. We have failed to detect any differences in the character of motion of TEC isolines on a quiet day 23 October 2003 and during the magnetic storm on 29 October 2003. Only a slight (about 30%) increase in the absolute value of velocity was observed at low latitudes. Thus, according to our calculations, the propagation of TEC isolines is determined by the Earth's diurnal rotation.

7. Discussion

[29] Global-scale investigation of TEC disturbances during the strong magnetic storm on 29 October 2003 has detected a wavelike LS TID which was continuously generated at the southern boundary of the auroral oval and traveled southwestward in the northern hemisphere. This result confirms the hypothesis that the source of ionospheric disturbances is situated in the auroral oval encircling the globe. *Ding et al.* [2007] studied LS TID in North America during the same storm on 29 October 2003 and came to the conclusion that the LS TID source likely to be located in the region (50–55°N; 70–80°W). It means that the source is situated at the southern boundary of the auroral oval (Figure 8). Our result is also in good agreement with data obtained earlier at ionospheric observatories during the October 1985 WAGS campaign [*Rice et al.*, 1988] and at a worldwide ionosonde network on 13 March 1989 [*Hajkowicz*, 1991].

[30] Comparison between LS TID propagation and the motion of TEC isolines shows that the diurnal movement of the ionization maximum may influence the zonal transfer of disturbance (Figure 9). The effect is especially strong near the terminator, where the variation of the electron density is most expressed. The zonal transfer manifest itself in shifting the LS TID annular wavefront relative to the geomagnetic pole.

[31] The westward deviation from the equatorward propagation direction of LS TID registered during magnetic storms has repeatedly been mentioned. We observed a westward displacement of LS TID propagation direction during a strong magnetic storm on 25 September 1998 using North America GPS network data [*Afraimovich et al.*, 2000]. The azimuth of the wave vector **K** varied along the wavefront from $\alpha = 245°$ at the longitude corresponding to 1600 LT to $\alpha = 177°$ at the longitude corresponding to 1900 LT. Toward the local nighttime, the propagation direction approached the equatorward direction. *Afraimovich et al.* [2000] reported the registration of a large-scale TEC disturbance in the southern hemisphere. This disturbance propagated equatorward, but a marked (by 30°) westward deviation of the direction must also be pointed out in this case. These results completely tally with data obtained in this paper.

[32] *Maeda and Handa* [1980], *Balthazor and Moffett* [1999], *Hall et al.* [1999], and *Foster et al.* [1989] provided numerical values for the LS TID propagation azimuth. They all mentioned a westward displacement of the azimuth, by 10–20° on average. The majority of the authors relate it to the Coriolis force effect on the AGW propagation in the atmosphere. Another way to explain such a structure of the disturbance wavefront was proposed by *Foster et al.* [1989]. According to *Foster et al.* [1989], the "swirling" of the disturbance front is the effect of a powerful stream of plasma ejected from rotating sunward polar cap. The issue of the reasons for the westward displacement of the LS TID propagation direction is still far from been resolved.

8. Conclusion

[33] The use of the GPS network and GPS radio interferometry methods developed by the authors made it possible to define the spatial structure and dynamic parameters of the LS TID generated during the strong magnetic storm on 29 October 2003. It was shown that the LS TID detected in the auroral zone after the SSC was a large-scale wave of the solitary type with an annular front whose center was located near the geomagnetic pole. The wave had a period of about 40–60 min and traveled up to 4500 km equatorward. The relative amplitude of LS TID calculated using the GIM data was 5–10%. Comparison with the ionosonde data has shown that this value corresponds to a relative amplitude of the electron density disturbance in the *F* layer maximum of about 45–50%. The LS TID occurred during a sharp change in the Earth's magnetic field.

[34] The velocity and travel direction of the LS TID had a strongly pronounced longitudinal dependence. A "swirling" effect was detected in LS TID propagation, with the "swirling" counter-directed to the Earth's rotation. The westward directed zonal component of the LS TID velocity caused this "swirling" effect. In the morning and evening sectors the zonal component exceeded the meridional one. The diurnal movement of the ionization maximum may influence the zonal transfer of LS TID.

[35] **Acknowledgments.** The work was supported by SB RAS collaboration project N 3.24 and RFBR grants 06-05-64577 and 08-05-00658. We acknowledge the Scripps Orbit and Permanent Array Center (SOPAC) for providing GPS data used in this study.

[36] Zuyin Pu thanks the reviewers for their assistance in evaluating this paper.

References

Afraimovich, E. L., E. A. Kosogorov, L. A. Leonovich, K. S. Palamarchouk, N. P. Perevalova, and O. M. Pirog (2000), Determining parameters of large-scale traveling ionospheric disturbances of auroral origin using GPS-arrays, *J. Atmos. Sol. Terr. Phys.*, *62*(7), 553–565, doi:10.1016/S1364-6826(00)00011-0.

Afraimovich, E. L., E. I. Astafieva, V. V. Demyanov, I. F. Gamayunov, T. N. Kondakova, S. V. Voeykov, and B. Tsegmed (2004), Ionospheric, geomagnetic variations and GPS positioning errors during the major magnetic storm on 29–31 October 2003, *Int. Ref. Ionosphere News*, *11*(3–4), 10–14.

Afraimovich, E. L., E. I. Astafieva, and S. V. Voeykov (2006), Generation of ionospheric irregularities under condition of solitary internal gravitational wave propagation during the major magnetic storm of 29–31.10.2003, *Radiophys. Quantum Electron.*, *49*(2), 79–104, doi:10.1007/s11141-006-0040-2.

Afraimovich, E. L., S. V. Voeykov, N. P. Perevalova, and K. G. Ratovsky (2008), Large-scale traveling ionospheric disturbances of auroral origin according to the data of the GPS network and ionosondes, *Adv. Space Res.*, *42*(7), 1213–1217, doi:10.1016/j.asr.2007.11.023.

Astafyeva, E. I., E. L. Afraimovich, and E. A. Kosogorov (2007), Dynamics of total electron content distribution during strong geomagnetic storms, *Adv. Space Res.*, *39*, 1313–1317, doi:10.1016/j.asr.2007.03.006.

Balthazor, R. L., and R. J. Moffett (1999), Morphology of large-scale traveling atmospheric disturbances in the polar thermosphere, *J. Geophys. Res.*, *104*(A1), 15–24, doi:10.1029/1998JA900039.

Ding, F., W. Wan, B. Ning, and M. Wang (2007), Large-scale traveling ionospheric disturbances observed by GPS total electron content during the magnetic storm of 29–30 October, 2003, *J. Geophys. Res.*, *112*, A06309, doi:10.1029/2006JA012013.

Foster, J. C., and W. Rideout (2005), Midlatitude TEC enhancements during the October 2003 superstorm, *Geophys. Res. Lett.*, *32*, L12S04, doi:10.1029/2004GL021719.

Foster, J. C., T. Turunen, P. Pollari, H. Kohl, and V. B. Wickwar (1989), Multi-radar mapping of auroral convection, *Adv. Space Res.*, *9*(5), 19–27.

Hajkowicz, L. A. (1991), Global onset and propagation of large-scale travelling ionospheric disturbances as a result of the great storm of 13 March 1989, *Planet. Space Sci.*, *39*, 583–593, doi:10.1016/0032-0633(91)90053-D.

Hall, G. E., J.-F. Cecile, J. W. MacDougall, J. P. St.-Maurice, and D. R. Moorcroft (1999), Finding gravity wave source positions using the Super Dual Auroral Radar Network, *J. Geophys. Res.*, *104*(A1), 67–78, doi:10.1029/98JA02830.

Ho, C. M., A. J. Mannucci, U. J. Lindqwister, X. Pi, and B. T. Tsurutani (1996), Global ionosphere perturbations monitored by the worldwide GPS network, *Geophys. Res. Lett.*, *23*, 3219–3222, doi:10.1029/96GL02763.

Hocke, K., and K. Schlegel (1996), A review of atmospheric gravity waves and traveling ionospheric disturbances: 1982–1995, *Ann. Geophys.*, *14*(5), 917–940.

Hofmann-Wellenhof, B., H. Lichtenegger, and J. Collins (1992), *Global Positioning System: Theory and Practice*, Springer, New York.

Klobuchar, J. A. (1987), Ionospheric time-delay algorithm for single-frequency GPS users, *IEEE Trans. Aerosp. Electron. Syst.*, *23*(3), 325–331, doi:10.1109/TAES.1987.310829.

Maeda, S., and S. Handa (1980), Transmission of large-scale TIDs in the ionospheric F2-region, *J. Atmos. Terr. Phys.*, *42*, 853–859, doi:10.1016/0021-9169(80)90089-6.

Mannucci, A. J., C. M. Ho, and U. J. Lindqwister (1998), A global mapping technique for GPS-derived ionospheric TEC measurements, *Radio Sci.*, *33*(3), 565–582, doi:10.1029/97RS02707.

Mannucci, A. J., B. T. Tsurutani, B. A. Iijima, A. Komjathy, A. Saito, W. D. Gonzalez, F. L. Guarnieri, J. U. Kozyra, and R. Skoug (2005), Dayside global ionospheric response to the major interplanetary events of October 29–30, 2003 "Halloween Storms,", *Geophys. Res. Lett.*, *32*, L12S02, doi:10.1029/2004GL021467.

Oliver, W. L., Y. Otsuka, M. Sato, T. Takami, and S. Fukao (1997), Climatology of F region gravity waves propagation over the middle and upper atmosphere radar, *J. Geophys. Res.*, *102*, 14,449–14,512.

Ratcliffe, J. A. (1959), *The Magneto-ionic Theory and Its Applications to the Ionosphere*, Cambridge Univ. Press, Cambridge, U. K.

Rice, D. D., R. D. Hunsucker, L. J. Lanzerotti, G. Crowley, P. J. S. Williams, J. D. Craven, and L. Frank (1988), An observation of atmospheric gravity wave cause and effect during the October 1985 WAGS campaign, *Radio Sci.*, *23*, 919–930, doi:10.1029/RS023i006p00919.

Zhao, B., W. Wan, and L. Liu (2005), Responses of equatorial anomaly to the October–November 2003 superstorms, *Ann. Geophys.*, *23*, 693–706.

E. L. Afraimovich, N. P. Perevalova, and S. V. Voeykov, Institute of Solar-Terrestrial Physics, Russian Academy of Sciences, SB RAS, 664033, P.O. Box 291, Irkutsk, Russia. (pereval@iszf.irk.ru)

I. V. Zhivetiev, Institute of Cosmophysical Research and Radiowave Propagation, Russian Academy of Sciences, FEB RAS, 684034, Mirnaya str., 7, Paratunka, Russia.